Computers and Biomedical Research **32,** 503–516 (1999)
Article ID cbmr.1999.1516, available online at http://www.idealibrary.com on IDEAL®

A Fuzzy Logic Approach to Identifying Brain Structures in MRI Using Expert Anatomic Knowledge

Gilbert R. Hillman,* Chih-Wei Chang,†,‡ Hao Ying,‡,§ John Yen,†
Leena Ketonen,¶ and Thomas A. Kent*,‖

**Department of Pharmacology, ‡Biomedical Engineering Center, and §Department of Physiology and Biophysics, University of Texas Medical Branch, Galveston, Texas 77555; †Department of Computer Science, Texas A&M University, College Station, Texas 77843-3112; and ‖Department of Neurology and ¶Department of Radiology, University of Texas Medical Branch, Galveston, Texas 77555*

Received November 18, 1997

We report a novel computer method for automatic labeling of structures in 3D MRI data sets using expert anatomical knowledge that is coded in fuzzy sets and fuzzy rules. The method first identifies major structures and then uses spatial relationships to these landmarks to recognize other structures. This labeling process simulates the iterative process that we ourselves use to locate structures in images. We demonstrate its application in three data sets, labeling brain MRI by locating the longitudinal and lateral fissures and the central sulci and then determining boundaries for the frontal lobes. Our method is adaptable to the identification of other anatomical structures.

Key Words: image segmentation; brain atlas; fuzzy logic; magnetic resonance images; functional MRI.

INTRODUCTION

As imaging technology has advanced, there has been great interest in associating neurological or psychiatric disease states with structural or functional anomalies that occur at specific locations in medical images (*1–8*). In order to use image data for colocalization with imaging of blood flow or metabolism, and for quantitative hypothesis testing, it is necessary to locate anatomical structures in the images: functional changes are typically restricted to a portion of the brain associated with a specific brain activity, such as a cognitive task, or a pathologic process, such as stroke. As this use of brain image analysis grows, there is widespread need for a method that identifies brain structures and allows them to be measured or to be registered with functional data.

Currently, the most widely used approach to identifying structures in images is by deforming, or "warping," standard images from a printed brain atlas (e.g., (*9*))

0010-4809/99 $30.00

to fit the target human brain images (*10, 11*), mapping structures from the atlas to the new images. More recently, a computer-based atlas has been developed that can deal with some of the variability among individuals in a probabilistic manner (*10*). Using visible features as tie points, the labeled standard image is deformed to register it with a given patient image, and the labels are then applied to the patient image on a point-by-point basis. This method has also proved particularly helpful in combining multiple image sets into an "average" image set (representing a population of patients with some condition, for example), for comparison of groups of patients. Newer versions of the warping method optimize the warping based on minimizing brightness differences globally (e.g., (*12*)), rather than using major features such as the boundaries of the brain to guide the warping process.

Accurately defining brain structures is difficult because of individual variability in brain anatomy. In the present work we suggest a novel fuzzy logic means to package expert knowledge of brain anatomy in such a way that the computer can use it to locate anatomical brain structures and their boundaries. Our method depends upon the fact that while structures vary among individuals in size, shape, and precise location, their general spatial relationships are predictable (*13*).

Motivated by the observation that many concepts in the real world do not have well defined boundaries, Zadeh (*14*) developed a fuzzy set theory that allows objects to belong partially to a set, whereas in traditional sets each individual object can have only "crisp" membership, i.e., it either belongs to a set or it does not. The degree to which an object belongs to a fuzzy set is given by a number between 0 and 1 and is called the membership value in the set; membership is defined by a "membership function," which permits one to calculate the degree to which any object is a member of the set. Fuzzy logic allows decisions, such as the identification of an anatomical structure, to be made on the basis of these partial memberships.

To illustrate how this works, imagine that we wish to identify the sternum in a skeleton. We make a fuzzy set, *sternum*, defined by membership functions for its vertical length (a few inches) and distance from the center of the chest (very short). Every bone in the body would have some membership in the *sternum* set, since they all have some vertical length and some distance from the chest, but when the membership in the *sternum* set is computed for every bone, one bone will have much higher membership than the others and we will choose that one as the sternum. This will still work even if an individual's sternum is atypical in some unexpected way, as long as it is not so abnormal that some other bone looks even more like a sternum. At the last step of the process (identifying one bone as the sternum) the fuzziness is removed, and the final identification is made crisp. This sort of decision-making, adapting itself to variations in the data, may be easy for trained humans to do, but is difficult to "explain" to computers. Fuzzy logic provides a way of presenting the process in terms that both humans and computers can understand (*15*)

Brain images can be analyzed by fuzzy logic because their general organization is predictable and well known but there is an expected amount of variation among individuals with respect to the sizes of structures and the distances and angles

between them. In the fuzzy system that we report here, knowledge of brain anatomy is encapsulated in fuzzy if–then rules, so that structures can be located and measured by their position relative to each other and to landmarks that can be identified reliably. Using membership functions, we express both the expected location of each structure of interest and the range of uncertainty of its location in any newly imaged individual.

In the present report we illustrate the use of our approach to locate the longitudinal fissure and the central and lateral sulci in three human brain data sets, leading to the location of the frontal lobes. We have chosen this problem because measurement of frontal gray and white matter volume is relevant to ongoing studies of head trauma and dementia, where frontal atrophy may occur (*16*). This capability should also be useful in other research projects, as the frontal lobes have been implicated in a variety of pathological processes (*17*). The present method should also be broadly adaptable to other imaging modalities and other anatomical structures (*18, 19*).

METHODS

The images were obtained on a GE Signa 1.5 T MR scanner using a head coil as the receiver. The images were T1-weighted gradient echo images (TR, 35 ms; TE, 5 ms; flip angle 35°), with 1.5 mm thickness, gap = 0, in coronal orientation. One subject studied had some brain atrophy, making the sulci wider and therefore their identification easier, but two other subjects had normal sulci; images from these subjects are used to illustrate all stages of the present method. We used an Indigo II Extreme workstation (Silicon Graphics, Inc.) and AVS graphics software (Advanced Visual Systems, Inc.) and wrote programs in C to implement the fuzzy and conventional image processing and 3D rendering. Most procedures could be completed in less than 30 min for one data set on the SGI computer.

We organize the process of localization as a sequential search. First we locate all sulci and fissures on the basis of image contrast. Next we locate landmarks that can be found unambiguously and easily: in the present example, the longitudinal fissure. Then, using fuzzy logic, we locate other structures on the basis of their position relative to the landmarks. In our example, we locate the central sulci and the lateral sulci, which are conventionally accepted as the boundaries of the frontal lobes. This method seems to us to model the way experienced viewers look at images, recognizing obvious structures first and identifying less obvious ones by their relationships to those already recognized. This apparent similarity to human image processing makes it easy to incorporate an expert's explanation of how to locate a particular structure.

Orientation and Interpolation of Data

Because the resolution in the interslice direction is lower than within the slices, we interpolated between the original 91 slices to create a $256 \times 256 \times 181$ image set, using simple linear interpolation. Interpolation adjusts the spacing between slices so that rendering the data as isotropic produces a realistic appearance and improves the apparent continuity of sulci where, because of their angle relative to

the slice plane, sulci that are truly continuous do not appear to occupy contiguous positions in adjacent slices.

The number of slices to be interpolated is chosen simply to make the data approximately isotropic. For the final rendering to appear strictly correct, the interpolated data set should be accurately isotropic: this could be achieved by interpolating variable numbers of new slices so that overall the number of slices per centimeter matched the number of pixels per centimeter within a slice (for example alternately interpolating 2 and 3 slices if $2\frac{1}{2}$ interpolated slices were really needed). However, for purposes of segmentation a simpler interpolation scheme is sufficient and we have used the uniform interpolation that produces the most nearly isotropic result. For our data, with pixel dimensions of about 1 mm and slice thickness of about 2 mm, we interpolated one slice between each original slice.

The angular orientation of the brain must be normalized because the apparent angle of the central sulcus, going from slice to slice, is sensitive to the position of the head relative to the slice angle. We observed that among images from a single MRI center the head angle usually does not vary much, but among images from different centers the slice angle differs substantially. Even at a single center the actual orientation of coronal slices depends on the patient's individual anatomy and the way the head is cushioned, but among many patients, correction of the angle might not be necessary if an effort was made to use a uniform head position when the data are acquired.

We use information in the mid-sagittal scout image, where the positions of the coronal images are shown. The anterior commissure and posterior commissure (AC and PC) are located by inspection and the angle between the coronal sections and the AC–PC line is measured. We have arbitrarily adopted an angle of 20° as "normal," and so data that is more than a few degrees away from this value is adjusted by resampling the interpolated data in new planes. Since only discrete resampling is possible, arbitrary rotational angles are not available, but a resampling pattern is selected that most closely approximates the necessary rotation. The detection of the central sulcus is based on a fuzzy description of its expected angle, so the amount of rotation of the data is not critical and need only approximately normalize the orientation of the slices.

Separation of Brain from Background

The background region of the image, outside the patient's head, is dark in all pulse sequences; the skull and CSF are also dark in the T1-weighted image. An interactive process is used to locate the brain tissue. Using the T1-weighted image, a threshold is applied; the value of the threshold can be varied by the operator. Whenever the threshold is changed, our program computes the areas of all regions of contiguous pixels above the threshold and displays only the largest such area; thus smaller areas representing the scalp, the meninges, and bright noise speckles are eliminated.

In some cases the meninges are so close to the brain surface that they appear connected to the brain and may connect the brain to the skull. In such cases an erosion algorithm is applied to remove one layer of pixels at a time, up to four

cycles of erosion, from the surface of the tissue above threshold. This process cuts the thin connections between the brain and the meninges and results in the isolation of the brain as the largest remaining object. An equal number of dilations is then applied to restore the brain to its original size.

A bounding box is computed surrounding the brain, a few pixels beyond the edges of the brain tissue. All subsequent computation is limited to the area within this bounding box.

Location of All Sulci

To recognize those pixels that belong to sulci in each 2D image, we use a modification of the fuzzy operator SURROUND (*15*). This operation identifies pixels that belong to one class (CSF) and are surrounded geometrically by another class (brain tissue).

The original definition of SURROUND defines a single angle over which an object is not surrounded by a second object: a value of 0 would indicate that one object is contained completely within another object in 2D space. We have modified this definition because in our case the CSF in a sulcus may be surrounded by more than one brain part, such as the frontal and temporal lobes. Our definition of SURROUND measures the number of degrees that are not covered by *any* objects that are not in the central pixel's class, within a square neighborhood of width w around the pixel in question. We apply this operator to each dark pixel, determining the extent to which it is surrounded by brighter brain pixels. Our version of the SURROUND operation (Fig. 1) for the sulci is defined to include pixels that are surrounded by more than π; i.e., pixels are considered to belong to a sulcus if more than half of the 360° surrounding them is occupied by brain, within a square neighborhood.

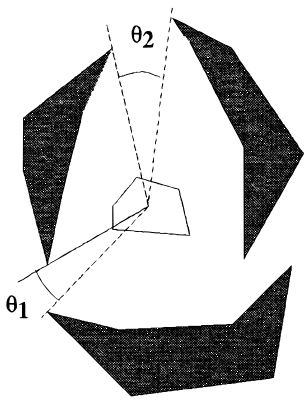

FIG. 1. Diagram illustrating the SURROUND operator. The region in the center is partially surrounded by three structures having a different composition than the central region. The angles θ_1 and θ_2 represent the portions of the imaginary circle surrounding the central region that are not occupied by the dark structures. The magnitude of SURROUND in this case is $360° - (\theta_1 + \theta_2)$.

The following expression determines the degree to which $p(\mathbf{x})$, a pixel, is surrounded by pixels in P, where P is a set of pixels:

$$\mu_{surround}\,(p(\mathbf{x}), P) = \frac{\int_0^{2\pi} f(p(\mathbf{x}), P, \theta)d\theta}{2\pi},$$

where

$$f(p(\mathbf{x}), P, \theta) = \begin{cases} 1, & \text{if } \exists\, \mathbf{y} \in P \wedge \mathbf{y} - \mathbf{x} \text{ has angle } \theta \\ 0, & \text{otherwise.} \end{cases}$$

We select pixels with a high degree of surround as follows:

$$\mu_{Massive-Surround} = \begin{cases} 2(\mu_{Surround}\,(p(\mathbf{x}), P) - 0.5), & \text{if } \mu_{Surround}(p(\mathbf{x}), P) \geq 0.5 \\ 0, & \text{otherwise.} \end{cases}$$

Any angle can be represented by θ; in Fig. 1 two values of θ are shown that illustrate ranges in which the central structure is not surrounded. The width of the neighborhood determines what regions are actually found by this process. If the width is large (e.g., (*25*)), pixels may be surrounded at a longer distance by brain and still be identified. In such a case pixels within the ventricles will also be found. However, if it is small (e.g., (*5*)), only pixels closely surrounded by brain will be found and therefore only surface sulci will be located. A byproduct of this property is that if the image were processed successively with the two values of the width and the results subtracted, the ventricles would be selectively located. The value of 5 was used for w in the studies described here. A computationally efficient algorithm was developed for computing the SURROUND function. Assigning contrasting colors to the brain and sulcal pixels and rendering background (empty) pixels as transparent, we can assemble the slices as a 3D rendering, as shown in Fig. 2.

Location of Specific Sulci

It is difficult to label specific sulci in individual 2D slices, as the sulci are seen only as a section in the plane of the image; this plane intersects with the sulci at angles and positions that are not exactly predictable. However, the general relative positions and orientations of the sulci in 3D space are known, and the range of likely locations for each major sulcus has been reported (*13*). In the case of a major sulcus, such as the longitudinal fissure, which runs perpendicular to the plan of the coronal images, it is possible to identify this sulcus in each 2D slice independently. For other sulci that are smaller or run at oblique angles, combined data from many slices must be used.

One fuzzy rule is defined to locate each sulcus of interest. Each rule combines

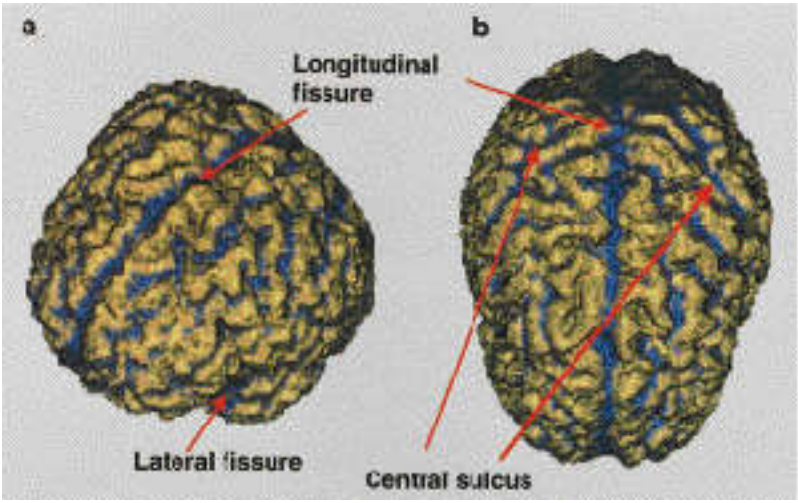

FIG. 2. Surface rendering of a brain from coronal slices, with sulci, determined by the SURROUND operator, colored blue. The same data set is shown from two points of view. The locations of the landmarks required for identification of the frontal lobes are also marked. The results of processing this same data set are shown in Figs. 4–7.

two or more fuzzy sets that capture the expert knowledge of the location and orientation of that sulcus, expressing it as a trapezoidal membership function; one example is shown below. The information contained in these fuzzy sets was sufficient for identification of the sulci, and no additional information was used. Since only one rule was used to identify each sulcus, no possible contradiction among rules can exist.

Longitudinal Fissure

Since the longitudinal fissure is located at the midline, it can be identified by calculating the distance of all sulcal pixels from the line that vertically bisects the bounding box that surrounds the brain in coronal sections; sulcal pixels near this line belong to the longitudinal fissure. For slices within the anterior third of the brain, this property alone is sufficient to identify longitudinal sulcus pixels. In slices more posterior, the longitudinal fissure is relatively shallow because the hemispheres are connected by the commissures, and the third ventricle is visible and may be incorrectly identified as a sulcus because it is a small region of CSF surrounded by brain. In these slices the positional rules must be modified to incorporate the fact that the longitudinal fissure is at the top of the brain. We define a fuzzy if–then rule to specify these conditions:

c IF *sulcus is close to the middle of the brain* AND *is close to the top of the brain* AND *is large* THEN *it is the longitudinal fissure*.

The rule above is used for the posterior two-thirds of the brain. Another rule without the clause involving *close to the top* is used for the anterior third. Each

of the three conditions indicated by underscores in this rule is a fuzzy set defined by a membership function. As an illustration of the membership functions that are used, we show the membership function for *close to the middle* in Fig. 3. These membership functions were constructed empirically, based on a medical expert's knowledge of anatomy, and communicated to a knowledge engineer who coded the information according to fuzzy logic formalities. In the rule, the word AND refers to Zadeh's fuzzy logic AND operator (*14*), which assigns the smallest of three memberships as the total degree to which the if condition is satisfied. The combined membership is then assigned to the rule consequent. All the fuzzy rules in our system were similarly derived, using fuzzy sets to capture the expertise of a neurologist, radiologist, or anatomist. After the pixels comprising the sulci have been located in all 2D slices by the thresholding process, the longitudinal fissure is labeled automatically according to these rules.

Central Sulcus

It is relatively difficult to identify the central sulcus in individual coronal slices because its direction is almost parallel to the coronal plane. The central sulcus therefore appears in only a few slices and in positions that sometimes are not obviously contiguous. It is easy to identify the central sulcus, however, once the sulcal fragments from all slices are assembled as a flattened surface map of the brain. The map is constructed by summing the SURROUND values along lines radiating from the center of the coronal section to the edge of the brain, at all angles from 0 to 360°; this sum is mapped to the surface where the line intersects it. This process is repeated for each coronal slice. The slices are assembled to form a 2D map representing the brain surface, as shown in Fig. 4. The anterior and

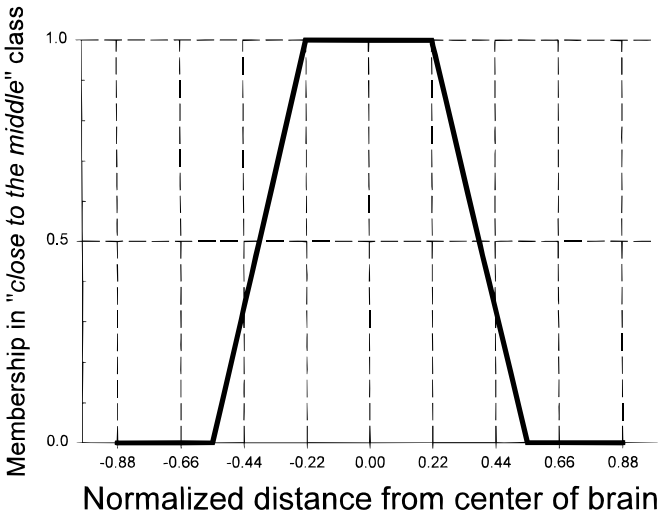

FIG. 3. Membership function for the *close to the middle* fuzzy set.

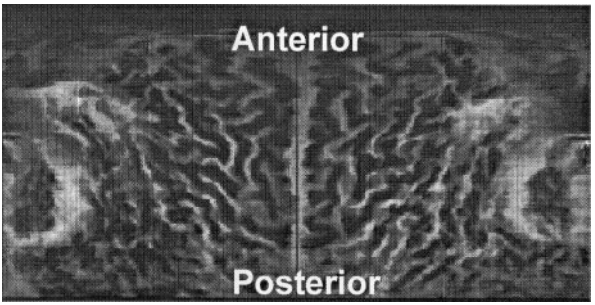

FIG. 4. Surface map of the brain, flattened onto a plane. Sulci are shown as lighter and gyri as darker.

posterior extremes of the brain are geometrically expanded by this transformation, which resembles a Mercator projection in mapmaking, but the location of the central sulcus is predictable within this distorted image. A morphological erosion operator is used to thin the sulci to a single pixel width, abstracting their structure as shown in Fig. 5. Pixels at the intersection of two sulcal branches are identified as "nodal" and are marked with dots.

The central sulcus is then identified by applying the following fuzzy rule to all sulcal pixels:

- IF *sulcus is near the middle of the brain* AND *is long* AND *has appropriate orientation THEN it is central sulcus*.

The *near the middle* degree is computed from the distance of any pixel from a line bisecting the bounding box of the brain. The degree of being *long* is computed relative to the entire set of all sulci: the longest sulcus found is normalized to length 1 and all others are expressed as fractional lengths.

The orientation of brain structures is often described relative to a coordinate system defined by the AC–PC line; the apparent angle of the central sulcus in a

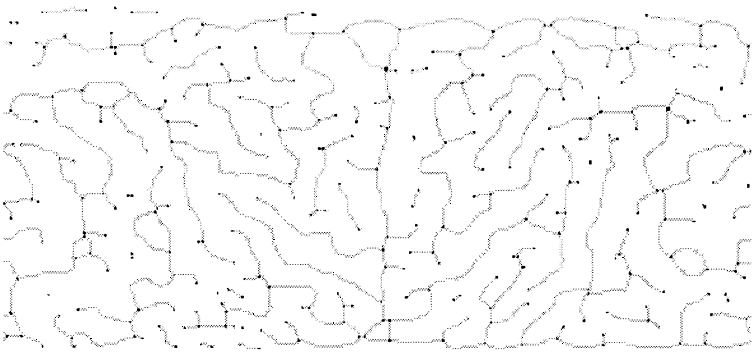

FIG. 5. Surface map with sulci thinned to a single pixel in thickness and with terminations and nodes marked with dots, permitting the length and orientation of each sulcus to be determined.

given data set depends on the orientation of the image slices relative to the actual brain anatomy. The images in our first data set are tilted about 20° from the AC–PC line, resulting in a predictable diagonal orientation (horizontal and slightly toward the front of the brain) of the central sulcus in the surface map just described. To identify sulci having this orientation we process the sulcal pixels using directional image filters that are designed to produce a positive response when positioned over a pixel that belongs to a line having a left-to-right upward slope from 0 to 45°.

Nodal pixels are not subjected to directional analysis but all nonnodal sulcal pixels are convolved with each of the four filters. If any one of the four filters produces a convolution value of 3 (i.e., three sulcal pixels fall under numerals "1" in the filter), then a nonzero membership value of *appropriate orientation* for that pixel is assigned. The assigned value is different according to which of the four filters matched the data: The filter closest to the expected orientation of the sulcus confers the highest membership value.

We collect the memberships of the component pixels of each sulcal segment in the surface map of the right hemisphere to determine the segment's overall direction. The procedure is repeated for the left hemisphere, with the orientation filters reversed.

The orientation memberships were combined with the length of the sulci and their location in the map, as stated in the fuzzy rule above, to give a membership in the central sulcus class. Figure 6 shows, as a color code, the membership values of several major sulci in the "central sulcus" class.

Lateral Sulci

The lateral sulci are long and run longitudinally near the bottom of the brain, sometimes connecting with the central sulcus. Based on these characteristics, we defined the following fuzzy rule to find the lateral sulci:

- IF *sulcus is close to the central sulcus* AND *has appropriate orientation* AND *is long* THEN *it is the lateral sulcus*.

The degree a sulcus is *close to the central sulcus* is computed by finding the minimum Euclidian distance from any pixel in the sulcus to any pixel in the already-identified central sulcus. Orientation filters are again used to select pixels belonging to sulci that run approximately parallel with the anterior–posterior axis of the brain.

This rule identified the lateral sulcus correctly according to expert observers. Since the anterior end of the lateral sulcus flares widely as it merges with the CSF surrounding the brain, the location of the end of the sulcus is somewhat arbitrary. Only the posterior, well-defined region of the lateral sulcus is required, however, to locate the lower boundary of the surface of the frontal lobes.

RESULTS

Having determined the surface boundaries of the frontal lobe (the lateral and central sulci), we locate the frontal lobe in 3D space by extending the central and lateral sulci inward to the midline. These inner boundary points could be adjusted according to an investigator's preference. Surface renderings for three data sets,

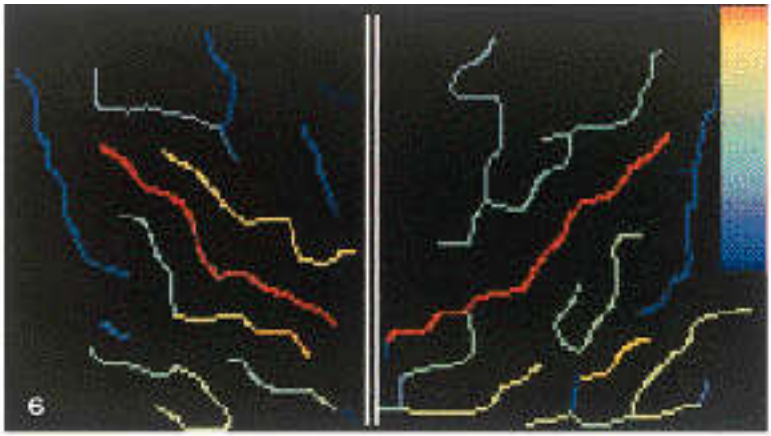

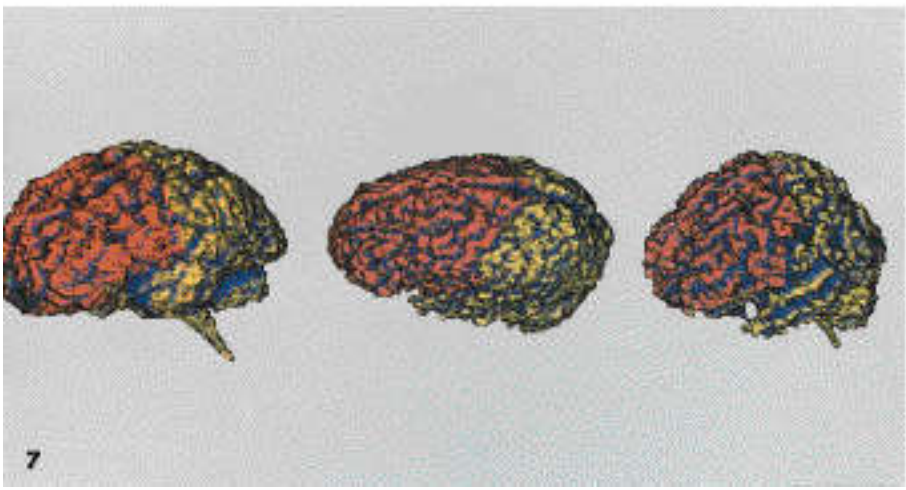

FIG. 6. Surface map showing major sulci, with a color code indicating the likelihood that each sulcus is the central sulcus according to the fuzzy rules. The scale ranges from blue (likelihood = 0) to red (likelihood = 1).

FIG. 7. Surface rendering of three brain MRI data sets, each processed to locate the frontal lobes, which are colored. The individual at the left had some generalized cortical atrophy, making the sulci more marked, but the other two brains were normal. The third example (right) was acquired with the head in a tilted position, causing some distortion in the apparent shape of the brain as rendered because of tile correction that was applied to permit analysis of the angle of the central sulcus.

one exhibiting some pathologic brain atrophy, is shown in Fig. 7 with the frontal lobes colored. The angle of the coronal sections in these data sets differed by about 20°. We adjusted the orientation membership functions of that data set (the rightmost one) accordingly; otherwise the processing was the same for all brains. Two expert observers indicate that the frontal lobes have been identified correctly in each case.

DISCUSSION

The process of identifying structures must proceed in two stages: first, one finds tissue that is an appropriate candidate for the structure being sought, and second, the correct choice is made among candidate regions. In the present example we first locate sulcal CSF and then decide which sulcus is a particular one that we wish to find. The present report emphasizes the identification of specific sulci by their location and geometric properties, once the set of all sulci has already been found. Fairly simple image processing is sufficient to locate CSF, as it contrasts strongly with brain tissue in T1- and T2-weighted images. In instances where there is not such obvious contrast it may require more effort to perform the preliminary tissue segmentation; a fuzzy logic-based technique for performing this task has been suggested (*20*). Others have also introduced methods for segmentation of individual MR images based on expert knowledge (*21–23*).

Our method for structure identification has two advantages that result from its automatic operation: it does not require an operator with anatomical expertise, and all critical judgments during the processing of a brain data set are made automatically, so that there is no interoperator variability in the results. The membership functions and fuzzy rules had to be constructed by experts, but once this task is completed the system is automatic. We consider the opportunity for expert input to be an advantage, since the complexity of brain structures precludes, in our opinion, the likelihood of recognizing interesting structures automatically without domain-specific knowledge.

We have demonstrated the use of fuzzy logic to encapsulate expert knowledge about 3D brain anatomy. A hierarchical process is used, in which an obvious structure (the longitudinal fissure) is identified first and then other structures are recognized by their positions relative to those already located. This method seems to mimic the way human experts identify objects in MR images: rather than comparing an image to a labeled standard, the expert looks for spatial relationships among familiar objects both within a slice and among adjacent slices. While it is not necessary for computer systems to mimic human thought processes, it is easier to capture a medical expert's knowledge as a computer algorithm if the algorithm mimics the expert's reasoning process as well as the outcome.

Our method is based on the assumption that there is enough interindividual similarity in the location of major brain structures to allow their automatic identification. A report from another laboratory of a successful method for identification of cortical sulci based on an understanding of interindividual variability (*13*) lends support to this assumption, and fuzzy logic has been used in the past to match MRI images to standard cortical topography (*24*).

Our method can be extended to automatic location of internal structures. Blurred

boundaries will have to be dealt with, but fuzzy segmentation programs should be capable of dealing with this (*15, 21*). In previously reported work (*25*), fuzzy membership functions were used to assign mixed membership to voxels containing both gray and white. We expect, based on the current results, that the present fuzzy expert system will be able to locate major brain structures in either normal or abnormal human brains as long as general spatial relationships are preserved. While it is necessary to develop fuzzy rules and fuzzy sets for each structure of interest, we suggest that the fuzzy logic system is so intuitive that anatomically oriented researchers will be able to use it easily to create expert systems for their own research purposes.

ACKNOWLEDGMENTS

The authors thank Professor Louis C. Sheppard for generous assistance. Some images were supplied by Dr. Harvey S. Levin, University of Maryland. Phillip Berryhill and Dr. Gerald Campbell provided additional anatomical expertise for identification of the frontal lobes. Image acquisition was supported by NIH NS-21889. Program development and research was supported in part by NIH R03 MH49552 and NSF IRI-9257293 and by the UTMB Center for Biomedical Engineering. This work was presented in part at ASNR 1996, at CFSA/IFIS/SOFT '95 on Fuzzy Theory and Applications Taipei, and at FUZZ-IEEE/IFES 1996

REFERENCES

1. Andreasen, N. C., Harris, G., Cizadlo, T., Arndt, S., O'Leary, D. S., Swayze, B., and Flaum, N. Techniques for measuring sulcal/gyral patterns in the brain as visualized through magnetic resonance scanning: BRAINPLOT and BRAINMAP. *Proc. Natl. Acad. Sci. USA* **91,** 93 (1994).
2. Andreasen, N. C., Arndt, S., Swayze, V., II, Cizadlo, T., Flaun, M., O'Leary, D., Ehrhardt, J. C., Yuh, W. T. C. Thalamic abnormalities in schizophrenia visualized through magnetic resonance image averaging. *Science* **266,** 294 (1994).
3. Fox, P. T., Perlmutter, J. S., and Raichle, M. E. A stereotactic method of anatomical localization for PET. *J. Comput. Assist. Tomogr.* **9,** 141 (1985).
4. Fox, P. T., Mikiten, S., Davis, G., and Lancaster, J. L. Brain map: A database of human functional brain mapping. *In* "Functional Neuroimaging Technical Foundations" (R. Thatcher, M. Hallett, T. Zefero, E. R. John, M. F. Huerta, Eds.), pp. 95–105. Academic Press, Orlando, FL, 1994.
5. Mazziotta, J. C. Physiologic neuroanatomy. New brain imaging methods present a challenge to an old discipline. *J. Cereb. Blood Flow Metab.* **4,** 481 (1984).
6. Huerta, M. F., Koslow, S. H., and Leshner, A. I. The Human Brain Project: An international resource. *Trends Neurosci.* **16,** 436 (1993).
7. Allen, G., Buxton, R. B., Wong, E. C., and Courchesne, E. Attentional activation of the cerebellum independent of motor involvement. *Science* **275,** 1940 (1997).
8. Calvert, G. A., Bullmore, E. T., Brammer, M. J., *et al.* Activation of auditory cortex during silent lipreading. *Science* **276,** 593 (1997).
9. Talairach, J., and Tournoux, P. "Co-planar Stereotactic Atlas of the Human Brain: 3-Dimensional Proportional System: An approach to Cerebral Imaging." Stuttgart: Georg Thieme Verlag. (1988).
10. Mazziota, J. C., Toga, A. W., Evans, A., Fox, P., Lancaster, A. Probabilistic atlas of the human brain: Theory and rationale for its development. *J. Neuroimage* **2,** 89 (1995).
11. Sandor, S., and Leahy, R. Matching deformable atlas models to preprocessed magnetic resonance brain images. *IEEE Int. Conf. Image Processing* **3,** 686 (1994).
12. Collins, D. L., Holmes, C. J., Peters, T. M., and Evans, A. C. Automatic 3-D model-based neuroanatomical segmentation. *Hum. Brain Mapping* **3,** 190 (1995).
13. Ono, M., Kubik, S., and Abernathey, C. D. "Atlas of the Cerebral Sulci." Thieme Medical, New York, 1990.
14. Zadeh, L. A. *Fuzzy Sets: Information Control* **8,** 338 (1965).

15. Krishnapuram, R., Keller, J. M., and Ma, U. Quantitative analysis of properties and spatial relations of fuzzy image region. *IEEE Trans. Fuzzy Syst.* **1,** 222 (1991).
16. Berryhill, P., Bruce, D., Brunder, D. G., Eisenberg, H. M., Fletcher, J. M., Hillman, G. R., Kent, T. A., Kufera, J., Lilly, M. A., Mendelsohn, D., Yeakley, J., and Levin, H. S. Frontal lobe changes after severe diffuse closed head injury in children: A volumetric study of MRI. *Neurosurgery* **37** (3), 392 (1995).
17. Levin, H. S., Eisenberg, H. M., and Benton, A. L. "Frontal Lobe Function and Dysfunction," pp. 92–121. Oxford Univ. Press, New York (1991).
18. Chang, C. W., Hillman, G. R., Ying, H., Kent, T. A., and Yen, J. Automatic labeling of human brain structures in 3D MRI using fuzzy logic. *In* "Proc. CFSA/IFIS/SOFT '95 on Fuzzy Theory and Applications, Taipei, Taiwan, pp. 27–34. 1995.
19. Chang, C. W., Hillman, G. R., Ying, H., Kent, T. A., and Yen, J. A fuzzy rule-based system for labeling the structures in 3D human brain magnetic resonance images. *In* "Proceedings FUZZ-IEEE/IFES 1996," pp. 1978–1982. 1996.
20. Chang, C. W., Hillman, G. R., Ying, H., Kent, T. A., and Yen, J. A two-stage human brain MRI segmentation scheme using fuzzy logic. *In* "Proceedings, FUZZ-IEEE 1995", pp. 649–654. 1995.
21. Bezdek, J. C., Hall, L. O., and Clarke, L. P. Review of MR Image segmentation techniques using pattern recognition. *Med. Phys.* **20**(4), 1033 (1993).
22. Raya, S. P. Low-level segmentation of 3-D magnetic resonance brain images A rule-based system. IEEE Trans. Med. Imaging **9,** 327 (1990).
23. Li, C., Goldgof, D. B., and Hall, L. O., Knowledge-based classification and tissue labeling of MR images of human brain. IEEE Trans. Med. Imag. **12,** 740 (1993).
24. Mangin, J. F., Regis, J., Frouin, V. Block, I. Regis, J. and Lopez-Krahe, J. From 3D magnetic resonance images to structural representations of the cortex topography using topology preserving deformations. J. Math. Imaging Vision **5,** 297 (1995).
25. Hillman, G. R., Kent, T. A., Kaye, A., Brunder, D. G., and Tagare, H. Measurement of brain compartment volumes in MR using voxel composition calculations. J. Comput. Assist. Tomogr. **15,** 640 (1991).